

THE OFFICIAL MAGAZINE OF THE OCEANOGRAPHY SOCIETY

Oceanography

CITATION

Wijesekera, H.W., W.J. Teague, E. Jarosz, D.W. Wang, T.G. Jensen, S.U.P. Jinadasa, H.J.S. Fernando, L.R. Centurioni, Z.R. Hallock, E.L. Shroyer, and J.N. Moum. 2016. Observations of currents over the deep southern Bay of Bengal—with a little luck. *Oceanography* 29(2):112–123, <http://dx.doi.org/10.5670/oceanog.2016.44>.

DOI

<http://dx.doi.org/10.5670/oceanog.2016.44>

COPYRIGHT

This article has been published in *Oceanography*, Volume 29, Number 2, a quarterly journal of The Oceanography Society. Copyright 2016 by The Oceanography Society. All rights reserved.

USAGE

Permission is granted to copy this article for use in teaching and research. Republication, systematic reproduction, or collective redistribution of any portion of this article by photocopy machine, reposting, or other means is permitted only with the approval of The Oceanography Society. Send all correspondence to: info@tos.org or The Oceanography Society, PO Box 1931, Rockville, MD 20849-1931, USA.

Observations of Currents Over the Deep Southern Bay of Bengal— With a Little Luck

By Hemantha W. Wijesekera, William J. Teague, Ewa Jarosz,
David W. Wang, Tommy G. Jensen, S.U.P. Jinadasa,
Harindra J.S. Fernando, Luca R. Centurioni,
Zachariah R. Hallock, Emily L. Shroyer, and James N. Moum



Photo credit: Hemantha Wijesekera

ABSTRACT. Long-term time series of velocity, hydrographic, and turbulence fields were collected from a six-element subsurface mooring array in the southern Bay of Bengal. The moorings, deployed in December 2013 and recovered in August 2015, were entangled with commercial fishing nets and lines, while top subsurface buoys ended up being serendipitously closer to the surface than planned. In spite of these unexpected events, almost all the sensors and data were recovered. The moorings provided currents between 6 m and 500 m depths from acoustic Doppler current profilers, supplemented by hydrographic data and turbulent dissipation rates at selected depths. The observations captured the summer and winter monsoon currents, eddies, and intraseasonal oscillations. Near-surface currents as large as 1.75 m s^{-1} were observed in July 2014. Currents stronger than 0.5 m s^{-1} were confined to the upper 200 m. Observations of currents, temperature, and sea surface height (SSH) fields revealed eddylike features with positive and negative SSH anomalies ($\sim 20 \text{ cm}$) moving westward at speeds of about 0.1 m s^{-1} . Intraseasonal oscillations with periods of 30 to 90 days were strongest near the surface. For the duration of the deployment, root-mean-square velocity fluctuations were about 0.1 m s^{-1} near the surface but decayed with depth and became nearly uniform ($\sim 0.03\text{--}0.06 \text{ m s}^{-1}$) below 100 m.

INTRODUCTION

Understanding the upper-ocean structure of the Bay of Bengal (BoB) and its connection to the entire northern Indian Ocean has been made more difficult by unknown freshwater distributions from high rainfall and river runoff. Several previous field campaigns focused on air-sea interaction and monsoon variability (e.g., Bhat et al., 2001; Murty et al., 1996; Webster et al., 2002; S.A. Rao et al., 2011). Bhat et al. (2001) conducted the Bay of Bengal Monsoon Experiment (BOBMEX) to examine organized convection during July–August 1999. Webster et al. (2002) addressed intraseasonal and interannual variability of the monsoon in the eastern Indian Ocean spanning 5°S to 15°N as part of the Joint Air-Sea Monsoon Interaction Experiment (JASMINE). S.A. Rao et al. (2011) led the Indian government research program Continental Tropical Convergence Zone (CTCZ), which examined intraseasonal variability and monsoon break cycles in the northern BoB during July and August 2009. Though these studies improved our understanding of ocean-atmosphere processes in the BoB, significant gaps in

our understanding remain. Determining the mixing pathways of river runoff and quantifying the upper-ocean heat and freshwater budgets are priorities because the shallow salinity-controlled mixed layers play a major role in the distribution of upper-ocean heat content and sea surface temperature (SST). Freshwater inputs and formation of shallow mixed layers are important for monsoon processes (Shenoi et al. 2002). Using historical hydrophysical fields, R.R. Rao and Sivakumar (2003) made an attempt to quantify the sea surface salinity budget.

Wind and remote equatorial forcing at the basin scale strongly control circulation and advection of saline waters (e.g., Yu et al., 1991; Potemra et al., 1991; Schott and McCreary, 2001; Shankar et al., 2002; Jensen, 2001, 2003; Vialard et al., 2009; Durland et al., 2009; R.R. Rao et al. 2010; Yu and McPhaden, 2011; Girishkumar et al., 2013; Suresh et al., 2013; Vinayachandran et al., 2013). The equatorial thermocline anomaly, generated by an eastward-propagating Wyrтки jet (Wyrтки, 1973) in response to westerly wind bursts (WWBs), propagates eastward as a free Kelvin wave.

Upon reaching the Sumatra coast, it partly reflects as a symmetric equatorial Rossby wave and two poleward-moving coastal Kelvin waves (e.g., Anderson and Rowlands, 1976; Cane and Sarachik, 1976; Philander, 1990). Northward-propagating Kelvin waves can move along the coastal boundary and influence circulation in the BoB. Analysis of satellite sea surface height (SSH) and direct current measurements along the east coast of India indicate that the alongshore currents in the upper-ocean flow field, especially near $15^{\circ}\text{N}\text{--}19^{\circ}\text{N}$, have strong intraseasonal oscillations (Vialard et al., 2009; Mukherjee et al., 2014).

Low-salinity BoB water is transported into the Arabian Sea (AS) via the East India Coastal Current (EICC) and the Winter Monsoon Current (WMC), and saltier Arabian Sea water is transported into the BoB via the Summer Monsoon Current (SMC; e.g., Murty et al., 1992; Schott et al., 1994; Shetye et al., 1996; McCreary et al., 1996; Schott and McCreary, 2001; Jensen, 2001, 2003; Durland et al., 2009; Vinayachandran et al., 2013; Mukherjee et al., 2014). The summer monsoonal forcing also induces energetic mesoscale features, which complicate the regional oceanographic circulation. Vinayachandran et al. (1999) suggested that the SMC east of Sri Lanka is forced by Ekman pumping in the BoB and Rossby wave radiation associated with the spring Wyrтки jet in the equatorial Indian Ocean. Recent shipboard and drifter observations reported by Wijesekera et al. (2015) reveal that low-salinity BoB water is removed from the bay by the EICC and that high-salinity water is transported into the BoB by a northward, subsurface-intensified flow east of the EICC. Model simulations and satellite products suggest that the WWBs over the equatorial Indian Ocean can be an important factor in the

BoB salinity balance during the north-east monsoon when saltier equatorial water intrudes into the southern BoB via a northward flow (Wijesekera et al., 2015). However, details of how upper-ocean processes control freshwater distribution and influence air-sea interactions are not well understood.

A better understanding of the spatio-temporal variability of currents and hydrophysical fields in the BoB as well as physical parameterizations that accurately capture relevant submesoscale and small-scale physics are required for accurate predictions of winds, sea surface temperature, and ocean currents by coupled air-sea models. The US Air-Sea Interactions Regional Initiative (ASIRI) directly addresses this problem. ASIRI focuses on regional-scale air-sea

interactions, atmospheric boundary layer structure, and ocean circulation in the BoB using both observations and models (Lucas et al., 2014; Wijesekera et al., in press). The US Naval Research Laboratory (NRL) program Effects of Bay of Bengal Freshwater Flux on Indian Ocean Monsoon (EBOB), in collaboration with ASIRI, focuses on two major objectives: (1) to understand and quantify dynamical processes and transports that control freshwater and saltwater exchanges between the BoB and the Southeast Arabian Sea, and (2) to examine ocean responses to buoyancy and wind-stress forcing using observations and high-resolution air-sea coupled models.

Observations of currents and hydrographic fields are required for assessing low-salinity water transports and the

role of mesoscale to small-scale dynamics in water mass exchanges as well as associated air-sea interactions on time scales ranging from subseasonal to seasonal. Currents in the southern BoB in a region east of Sri Lanka, especially in the thermocline and below, are a mystery due to lack of long-term in situ observations. As a part of the EBOB observational component, NRL Oceanography Division scientists, in collaboration with Oregon State University (OSU), the University of Notre Dame (ND), and the National Aquatic Research and Resources Development Agency (NARA) in Sri Lanka, deployed six deep subsurface moorings in the southern BoB (Figure 1). In collaboration with Scripps Institution of Oceanography (SIO), several drifters were also deployed near the mooring

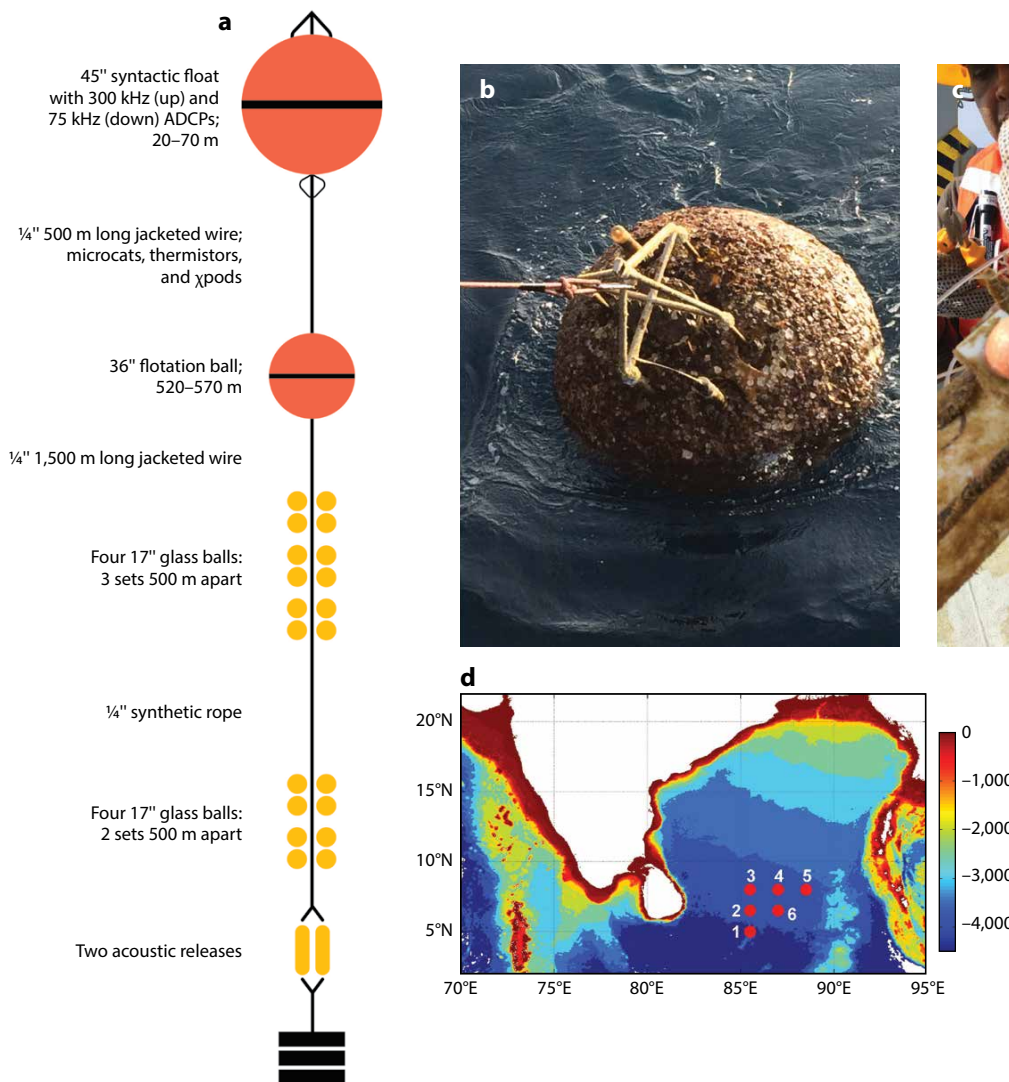


FIGURE 1. (a) Schematic of the mooring configuration. (b) The top acoustic Doppler current profiler (ADCP) ball of NRL3 during recovery shows heavy biological growth due to placement of the ball as shallow as 16 m (Table 1). (c) Entanglement of mooring components with fishing nets and lines. (d) Locations of US Naval Research Laboratory (NRL) moorings 1–6 marked in red bullets over a bathymetry map of the Bay of Bengal (color image).

array to capture near-surface circulation. These new long-term high-resolution observations help quantify a range of motions, including seasonal and intra-seasonal currents, eddies, internal waves, and tides originating from the Andaman-Nicobar Island gaps. Here, we describe the initial findings of low-frequency currents observed from the mooring array.

MEASUREMENTS

The observational program consisted of a 20-month-long mooring deployment, from December 2013 to August 2015, and a 10-day intensive survey period from July 3–13, 2014, using a towed undulating vehicle, ScanFish, in the upper 150 m. Six moorings were deployed in a triangular array (5°–8°N, 85.5°–88.5°E) in the southern BoB (Figure 1) using R/V *Roger Revelle* operating from Colombo, Sri Lanka. All six moorings were deployed in international waters at depths of 3,600–3,900 m (Figure 1, Table 1). The western edge of the mooring array was approximately 370 km east of Sri Lanka, and the separation between adjacent moorings was approximately

167 km. The mooring line NRL1-2-3, along 85.5°E, provided meridional cross sections of currents and hydrographic fields, and the mooring line NRL3-4-5, along 8°N, provided zonal cross sections. The moorings were deployed in a transition region where the northern end of the array was influenced by the low-salinity northern BoB flow field, while the southern end was influenced by the high-salinity southern Arabian Sea equatorial flows and the dynamics of the equatorial waveguide. Furthermore, the moorings were placed in the path of tidal beams radiating from the shallow gaps between Andaman and Nicobar Islands near 93°E, 9°N.

Each mooring contained two acoustic Doppler currents profilers (ADCPs) mounted on a buoy. In addition, each mooring contained 12–14 temperature (T) sensors; three to four temperature and conductivity (TC) sensors and four to six temperature, conductivity, and pressure (TCP) sensors; two turbulent sensor packages (χ pods, see Science Box 1); two acoustic releases; a 0.9 m (36 inch) diameter flotation ball; and 20 glass

flotation balls (Figure 1). The ADCPs were mounted upward and downward looking in a 1.143 m (45 inch) diameter top-buoy (hereinafter referred to as ADCP ball), and the rest of the sensors were attached to the 500 m long, 6.35 mm (0.25 inch) jacketed steel wire below the ADCP ball (Figure 1). The vertical position below the water surface of the ADCP ball varied from 16 m to 72 m (Table 1), even though planned locations were 60–70 m below the water surface. The upward-looking 300 kHz ADCP recorded velocity profiles in the water column from the top of the ADCP ball to about 5 m below the water surface every 30 minutes, and the downward-looking 75 kHz ADCP recorded velocity profiles in the water column to about 500 m below the ADCP ball every one hour (Table 1). Accuracies for the ADCP velocity measurements are 0.5% of the observed water velocity $\pm 0.5 \text{ cm s}^{-1}$. T, TC, and TCP sensors sampled at 1 min and 10 min intervals, respectively. The χ pods located at 10 m and 30 m below the ADCP ball recorded temperature, pressure, and acceleration at 100 Hz to determine temperature variance dissipation rates. The

Table 1. Acoustic Doppler current profiler (ADCP) mooring summary. The 300 kHz ADCP was upward looking and the 75 kHz ADCP was downward looking. Zbuoy is the depth of the top buoy or the ADCP ball. H is the water depth. Δt is the sampling period of ADCPs. Z1, Zn, and Δz are the depth of the first bin, the depth of the last bin, and the bin size, respectively. All depths are in meters. T_f is the inertial period in days. Start day and end day are given as month/day for 2013 and 2015, respectively. The site locations of NRL moorings 1–6 are marked with red bullets in Figure 1d.

Site	Lat (°N)	Lon (°E)	Start (day)	End (day)	Δt (min)	Z1 (m)	Zn (m)	Δz (m)	Zbuoy (m)	H (m)	Type (kHz)	T_f (days)
NRL1	5.009	85.511	12/19	8/06	30	6	134	2	44	3715	300	5.711
			12/19	8/06	60	64	592	8		75		
NRL2	6.500	85.500	12/19	8/07	30	6	106	2	39	3876	300	4.405
			12/19	8/07	60	56	768	8		75		
NRL3	8.000	85.500	12/20	8/08	30	6	126	2	16	3757	300	3.583
			12/20	8/08	60	32	592	8		75		
NRL4	7.992	86.990	12/21	8/09	30	6	142	2	45	3678	300	3.586
			12/21	8/09	60	64	576	8		75		
NRL5	7.983	88.500	12/21	8/10	30	6	166	2	72	3638	300	3.590
			12/21	8/10	60	88	624	8		75		
NRL6	6.500	87.000	12/22	8/11	30	6	112	2	59	3840	300	4.405
			12/22	8/11	60	80	576	8		75		

Science Box 1. Moored Mixing Measurements in the Bay of Bengal

Resolution of seasonal variability associated with strong forcing on monsoonal time scales requires full-year records of turbulent heat flux. The ASIRI project has supported collection of multiyear records of mixing throughout the Bay of Bengal using moored χ pods (Figure SB1). Five of the six NRL moorings were equipped with two χ pods each from December 2013 to June 2015, and additional sensors were deployed on RAMA moorings at 12°N and 15°N from December 2013 to December 2015 and on an air-sea flux mooring near 18°N from November 2014 to January 2016. The χ pods measure mixing using fast thermistors (Moum and Nash, 2009; Perlin and Moum, 2012), which sample temperature fluctuations at 100 Hz. Frequency spectra are converted to wavenumber spectra using the local speed from ancillary sensors (e.g., ADCPs); wavenumber spectra are scaled to estimate the diffusive rate based on the turbulent thermal dissipation rate (χ). The turbulent diffusivity of temperature (K_T) and the viscous rate of dissipation of turbulence (ϵ) are derived from χ under the assumptions that (1) the diffusivity of temperature is equivalent to the diffusivity of density, and (2) the mixing efficiency is 20%.

Despite challenges associated with estimation of background temperature gradients from moored data and errors in current speed past the sensor due to mooring motions, χ pods provide the only vetted (Perlin and Moum, 2012), continuous, year-round measurements of turbulent mixing on moored platforms, permitting the sampling needed to capture intermittent turbulent events and providing statistically robust average mixing rates. Furthermore, the flexibility of these sensors has been demonstrated through adaptation to CTD rosettes, Wirewalker profilers, and SOLO-II profiling floats. For example, data collected from a CTD-mounted χ pod in November–December 2013 show mixing that was likely enhanced by Tropical Cyclone Madi, which occupied the region just offshore of Sri Lanka in the weeks preceding the deployment of the NRL mooring array. The turbulent thermal dissipation rate (χ) was elevated by several orders of magnitude over background values. The ~ 1.5 year-long records of mixing from NRL array χ pods will permit quantification of the intensity and variability in mixing associated with the passage of multiple storms and energetic eddies such as the Sri Lanka Dome. The data shown in Figure SB1 suggest that such storm events may be responsible for significant subsurface mixing in the BOB.

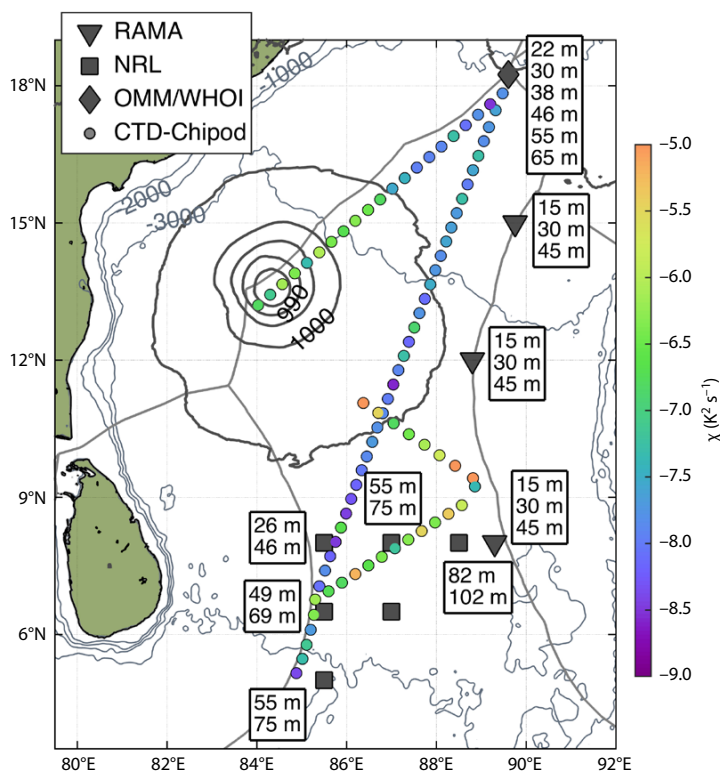


FIGURE SB1. Locations of moored χ pods deployed for ASIRI. Boxes closest to mooring positions indicate nominal depths of sensors. Each small colored circle shows the location and magnitude of an average thermal dissipation rate (χ) in the upper 250 m as calculated from a χ pod mounted on a CTD. Profiles were acquired from November 29 to December 11, a period spanning the development of Cyclone Madi (sea level pressure field in millibars from December 9, 2013, thick black lines). The thick gray and thin black lines denote Exclusive Economic Zone (EEZ) boundaries and bathymetric contours, respectively.

locations and the numbers of χ pods used in moored platforms, and the estimated temperature variance dissipation rates from a ship CTD-mounted χ pod along the cruise track of R/V *Roger Revelle*, are given in Science Box 1. T, TC, and TCP sensors were spaced unevenly within 500 m below the ADCP ball. Sensors were dense in the strongly stratified region between 50 and 150 m.

During the deployment period, mooring motion generated large vertical displacements ranging from 10 m to 150 m as indicated by the pressure records of the ADCPs and TCP sensors. These displacements varied with tides as well as low-frequency currents, and on several occasions displacements as large as 150 m occurred that lasted more than a month. At least three of the six moorings were entangled with commercial fishing nets and lines (Figure 1), which in turn generated extra drag on the mooring lines, and could have caused unexpected displacements. However, tilt sensors in the ADCPs indicated that the ADCPs were nearly vertical and that the mooring motion had little impact on the vertical orientation of the subsurface buoy. The ADCP ball was connected to the mooring line through a swivel/shackle/master-link assembly that decoupled the vertical orientation of the mooring line from the ball. Here, for a given a mooring, depths of velocity bins were referenced relative to the ADCP pressure. T, TC, and TCP sensors were rigidly attached to the mooring line, so their vertical positions were directly affected by the tilt of the mooring line. Pressure levels at T and TC sensor locations were evaluated by interpolating the pressure records of the ADCPs and the TCP sensors. ADCP current and temperature fields were corrected to the mooring motion, and a gridded product was constructed by interpolating ADCP currents and temperatures to constant depth levels between 8 m and 500 m with 8 m and 4 m depth intervals, respectively. Salinity was limited to four to six sensors at each mooring and therefore was not interpolated vertically.

PRELIMINARY ANALYSIS AND RESULTS

The time series of currents and hydrographic fields comprised two winter monsoon and two summer monsoon seasons between December 2013 and August 2015. Multiple events at a range of temporal and spatial scales passed through the mooring array as illustrated in time-longitude plots of SSH (Figure 2). One of the distinct features is the annual and seasonal cycles of SSH. Here, daily products of SSH anomalies from the Aviso data set with $\frac{1}{4}^\circ$ spatial resolution (<http://www.aviso.altimetry.fr/en/data/products/sea-surface-height-products/global/ssha.html>) were used. From May to September 2014, SSH anomalies as large as ± 25 cm propagated westward at a speed of about 0.09 m s^{-1} , which

is close to the theoretical phase speed of the second-mode baroclinic Rossby wave speed for the latitude belt near 8°N (e.g., Figure 1 in Subrahmanyam et al., 2001). Note that the slopes of the longitude-time plots of SSH are the propagation speeds. The monthly averaged SSH image shown in Figure 3 displays the spatial structure of mesoscale variability in the southern BoB for July 2014. The image shows well-developed cyclonic (negative SSH anomaly) and anticyclonic (positive SSH anomaly) mesoscale features approximately 300–400 km long and 200–300 km wide. The cyclonic circulation east of Sri Lanka, which appears during the summer months, is referred to as the “Sri Lanka Dome” (e.g., Vinayachandran and Yamagata, 1998).

The seasonally reversing wind patterns

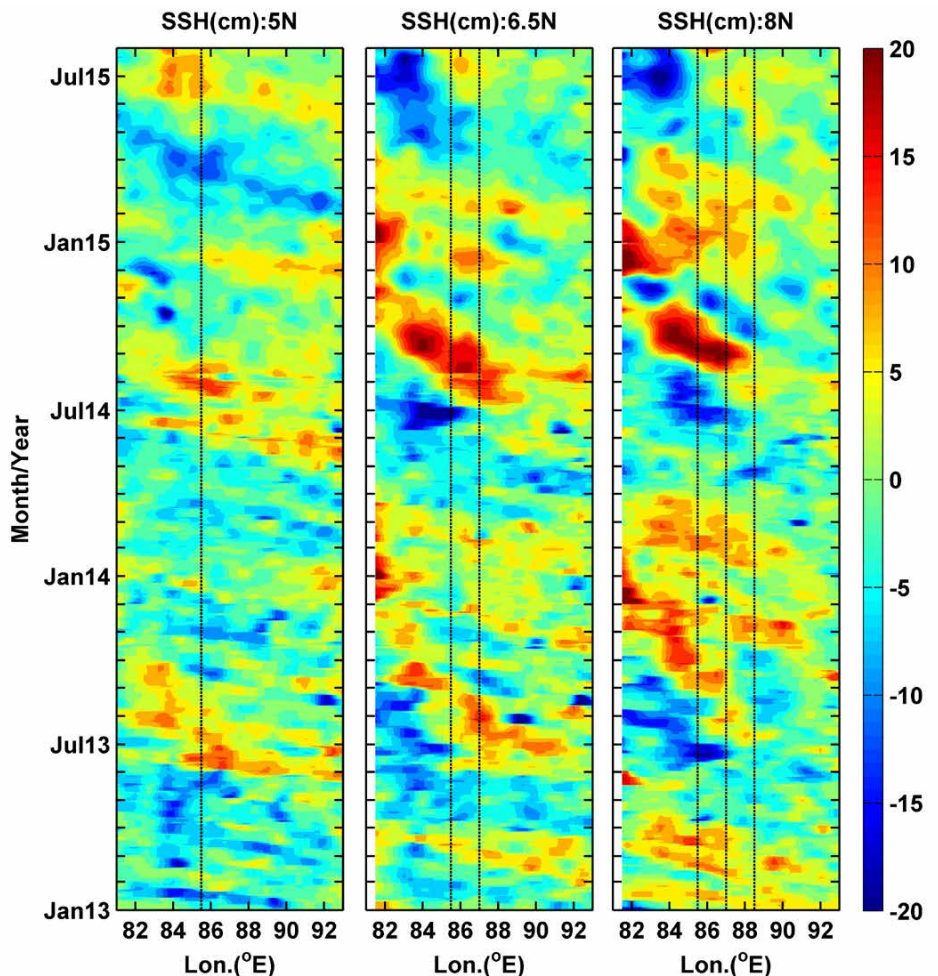


FIGURE 2. Longitude-time (Hovmöller) diagrams of sea surface height (SSH) anomaly at 5°N (left), 6.5°N (middle), and 8°N (right). Thin black lines indicate the NRL mooring locations. SSH is in centimeters.

in the central BoB were remarkably steady during the period of mooring deployment (Figure 4a). The 10 m winds were from the Research Moored Array for African-Asian-Australian Monsoon Analysis and Prediction (RAMA) buoy at 12°N, 90°E (McPhaden et al., 2009). The 20-day low-passed filtered winds during the southwest monsoon were about 10 m s^{-1} . The southwest monsoon winds were stronger than the northeast monsoon winds, which were about 6 m s^{-1} . The transitions from northeast to southwest monsoons, and vice versa, occurred in May and October, respectively, and these wind reversals each took place within a month (Figure 4a).

The SSH anomaly followed the 20°C isotherm depth extremely well throughout the deployment (Figure 4b). The correlation coefficient between the 20°C

isotherm and SSH is about 0.84 at NRL3. Similar correlations are found at the rest of the mooring sites where correlation coefficients at NRL1, NRL2, NR4, NRL5, and NRL6 are 0.75, 0.75, 0.84, 0.69, and 0.82, respectively. The 20-day low-passed filtered 20°C-isotherm depth shown in Figure 4b was derived from 10 min and 4 m averaged gridded temperature observations. Here, negative SSH anomalies (i.e., counterclockwise circulation) and positive SSH anomalies (i.e., clockwise circulation) were highly correlated with upward and downward movement of the thermocline, respectively. The time-depth section of temperature (Figure 4d) shows that vertical movement of isotherms occurred throughout the water column, especially during the summer of 2014 (Figure 4b,d). The near-surface temperature was warmest at

about 30.5°C at 16 m depth during April and May (Figure 4d), especially prior to the southwest monsoon.

Salinity near the surface (~20 m) was about 33.5 psu or less, except in the cold, cyclonic Sri Lanka Dome eddy (Figure 4c). The Sri Lanka Dome, observed in July 2014, was associated with cold and slightly higher-salinity water and with rising isotherms. The anticyclonic eddy, observed in September 2014, was associated with warm water and deepening isotherms (Figure 4b,d). Typically, the low-saline, warm water can lead to a positive SSH anomaly, but the relative contributions of these two components determine SSH variability. Because our salinity measurements are very limited, it is difficult to evaluate the relative contributions of temperature and salinity in cyclonic and anticyclonic eddies. Based on historical expendable bathythermograph (XBT) measurements along 6°N between 80°E and 95°E, Yu (2003) reported that the amplitude of the SSH anomaly (~3 cm) induced by the salinity is comparable to the amplitude induced by temperature. Salinity in the deeper part of the thermocline remained steady in time. Salinities at 10 min intervals were plotted on the observed pressure levels due to the limited number of salinity observations (Figure 4c). Pressure records of individual sensors reflect the vertical movement of the mooring. Tilting of the NRL3 mooring when monsoon currents were strong in summer 2014 caused 50–75 m vertical displacements. In June 2015, the mooring moved more than 150 m vertically for nearly a month even though the currents were not large. Short-duration displacements can be found throughout the deployment period. We suspect that the large displacements could be a result of fishing-net entanglement, which tends to drag the mooring line.

In general, currents at all the mooring sites show rapid responses to reversing wind fields, and these changes are more pronounced at NRL3. The time series of currents at NRL3 (Figure 4e,f) displays the seasonal response to monsoons. In

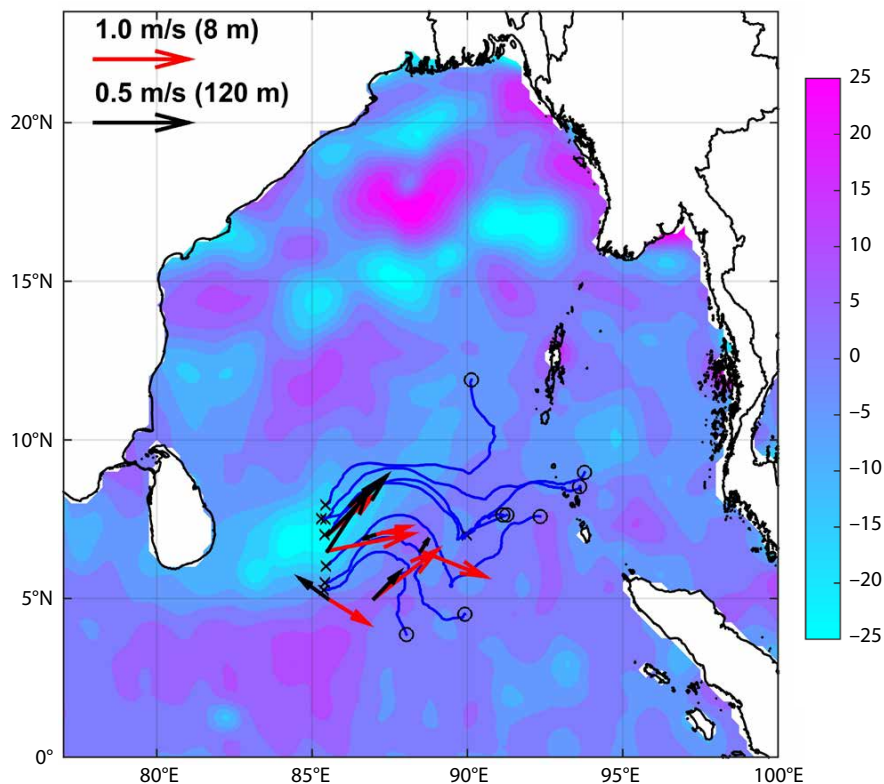


FIGURE 3. Summer monsoon currents from drifters and moored ADCPs are superimposed on an SSH map for July 2014 (color image). SSH is in centimeters. Drifter velocity vectors for the middle of July 2014 are marked by blue lines. Starting and ending points of drifters are marked by crosses and circles, respectively. ADCP current vectors at 8 m and 120 m depths are marked by red and black arrows, respectively. The current vectors at 120 m were multiplied by a factor of two. Currents at 120 m depth were more directed northward.

general, low-frequency currents in the upper 100 m were in excess of 0.6 m s^{-1} (Figure 4c). The strongest currents were observed during the southwest monsoon (July–August 2014). The monthly averaged near-surface zonal flow exceeded 1 m s^{-1} while the meridional flow contained subsurface maxima of about 0.6 m s^{-1} at 50–100 m depth. The summer monsoon circulation observed during June–August 2014 at NRL3 showed passages of energetic cyclonic and anticyclonic eddies apart from the SMC. Mean currents observed during northeast monsoon periods (December–March) were less than 0.1 m s^{-1} , nearly westward,

and shallow (confined to upper 100 m). Below 200 m, currents were dominated by wavelike motions with time periods varying from 30 to 90 days.

Seasonal currents were strong in the upper 200 m while seasonal currents were weak below 200 m, but intraseasonal oscillations were significant. Therefore, the temporal variability of currents was further examined by depth averaging the zonal and meridional velocity components into two separate depth intervals, namely 8–200 m and 208–500 m (Figure 5). Immediately after the southwest monsoon, the upper 200 m flow, especially at NRL moorings 1–4, intensified

toward the northeast. However, it is likely that a part of the wind-driven flow was heavily influenced by cyclonic and anticyclonic eddy structures during June–July 2014 (Figures 3, 4, and 5). As mentioned above, the Sri Lanka Dome is a result of Ekman pumping in the southern BoB. Note that the Ekman pumping, estimated from Coupled Ocean/Atmosphere Mesoscale Prediction System (COAMPS) model outputs (<http://www.nrlmry.navy.mil/coamps-web/web/home>) near 84°E – 85.5°E , 8°N – 9°N during June–July 2014 is about 1 – 2 m day^{-1} . The anticyclonic circulation is likely associated with Rossby waves radiating from the

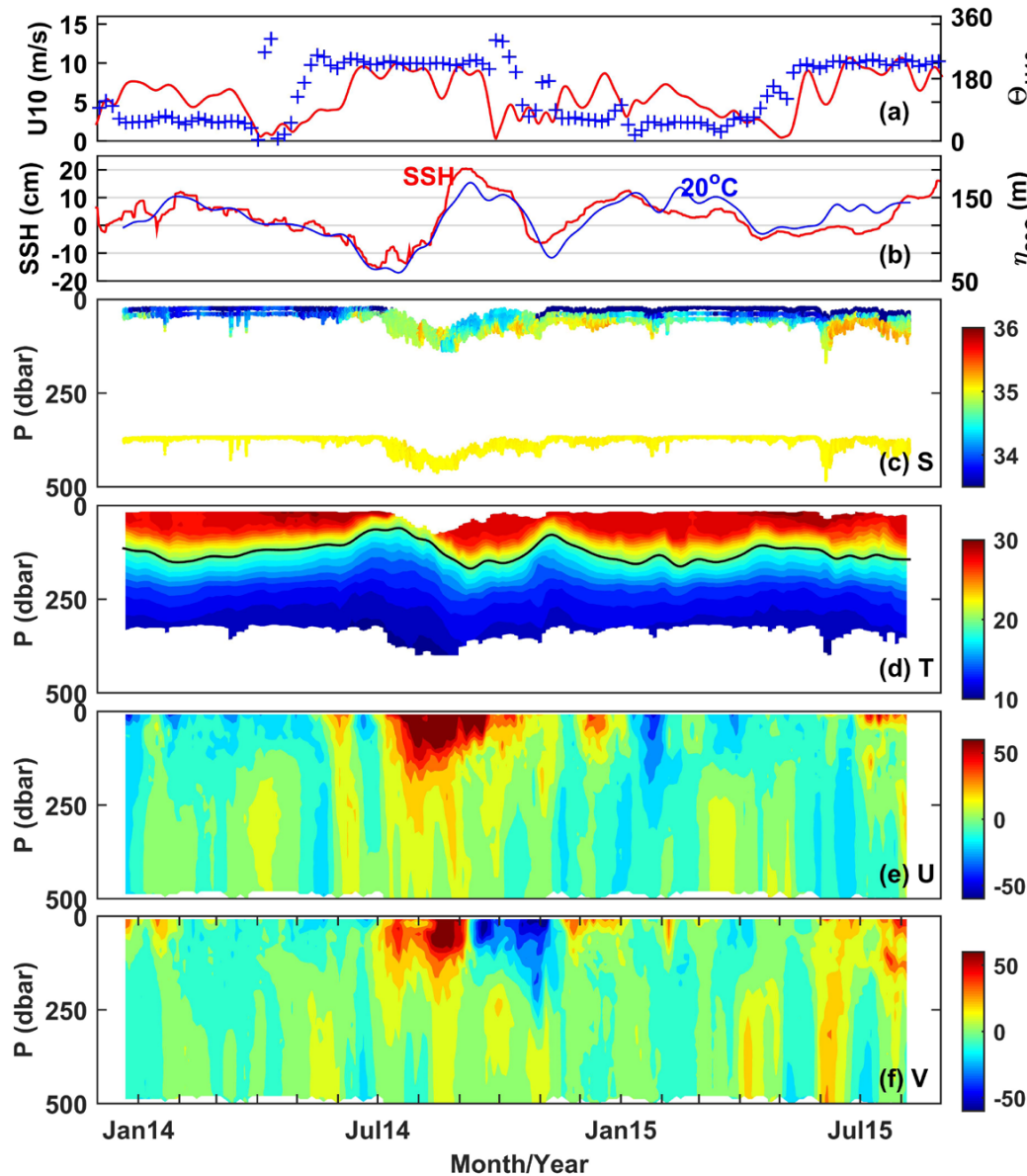


FIGURE 4. Current, temperature, and salinity observations at mooring NRL3 (85.5°E , 8°N). (a) 10 m wind speed and direction from meteorological sensors mounted on the RAMA buoy at 90°E , 12°N . (b) SSH anomaly (red) from Aviso and 20°C isotherm depth (blue) at the mooring location. (c) Scatter plots of 10 min sampled salinity (S) at five depths along the mooring line. Seventy-two-hour low-pass filtered (d) temperature (T) in $^{\circ}\text{C}$, (e) zonal velocity (U), and (f) meridional velocity (V).

eastern boundary (e.g., Vinayachandran et al., 1999). In August–September 2014, the mooring array captured this westward-moving anticyclonic feature, which is consistent with the reversal of the flow toward the southwest (Figures 4 and 5). The time-mean currents below 200 m were weak but dominated by subseasonal oscillations (Figure 5). There is a weak northward flow at NRL3 throughout the 20 months of observations, while the zonal flow reverses subseasonally. The cumulative velocity estimates indicate a subsurface northward transport at the western edge of the mooring array.

The surface circulation pattern

observed in July 2014 from drifter tracks and from the moored ADCPs is qualitatively consistent (Figure 3). The tracks of eight surface drifters deployed July 3–5 along the NRL1–3 mooring line from R/V *Roger Revelle* are marked by blue arrows. Directions of moored ADCP velocities at 96 m to 120 m depth are marked by red and black arrows, respectively. The near-surface flow pattern closely followed SSH contours in the southern BoB during August 2014. After the passage of these eddies, many of the drifters moved eastward toward the Andaman Sea, and only one out of eight drifted to the northern BoB, indicating

that the surface transport was mostly eastward. However, between 50 m and 125 m depths, the subsurface flow had a strong northward component of about 0.5 m s^{-1} during June–August 2014 and July 2015 (Figures 3 and 4f), and was associated with salinity higher than 35 psu (Figure 4c). It has been recognized that the SMC transports the major influx of saltier water into the BoB from the southeast Arabian Sea (e.g., Murty et al., 1992; Schott and McCreary, 2001; Vinayachandran et al., 2013). Since the surface-intensified SMC moved eastward, it is likely that the subsurface-intensified northward component of the flow carried high-salinity water into the northern bay.

Low-frequency SSH anomalies propagated westward at a speed close to 0.09 m s^{-1} (Figure 2). Furthermore, SSH anomalies were highly correlated with the 20°C isotherm depth (Figure 4b). This observation implies that wave- or eddy-like disturbances in the thermocline propagated westward. The 90-day low-passed filtered 20°C -isotherm displacements and the depth-averaged meridional velocities at NRL2–6 show phase lags in the zonal direction among NRL3, NRL4, and NRL5 and between NRL2 and NRL6 (Figure 6). By matching 20°C isotherms of nearest mooring locations and also matching meridional velocities at 6°N , we found 8- to 14-day time lags for 20°C isotherms and a 20-day time lag for the velocity fields. At 8°N , we found 10- to 20-day time lags for isotherms and 25- to 30-day time lags for the velocities. We note that our time-lag estimates have large uncertainties due to latitudinal dependence of the propagation speed, so an average speed was estimated. The average, minimum, and maximum propagation speeds are about 0.12 m s^{-1} , 0.06 m s^{-1} to 0.24 m s^{-1} , respectively. These results are similar to the propagation speeds derived from the SSH anomalies discussed above (Figure 2). Yu (2003) reported westward propagation of the 20°C isotherm from XBT measurements along 6°N between 80°E and 95°E . The estimated phase speed from the XBT

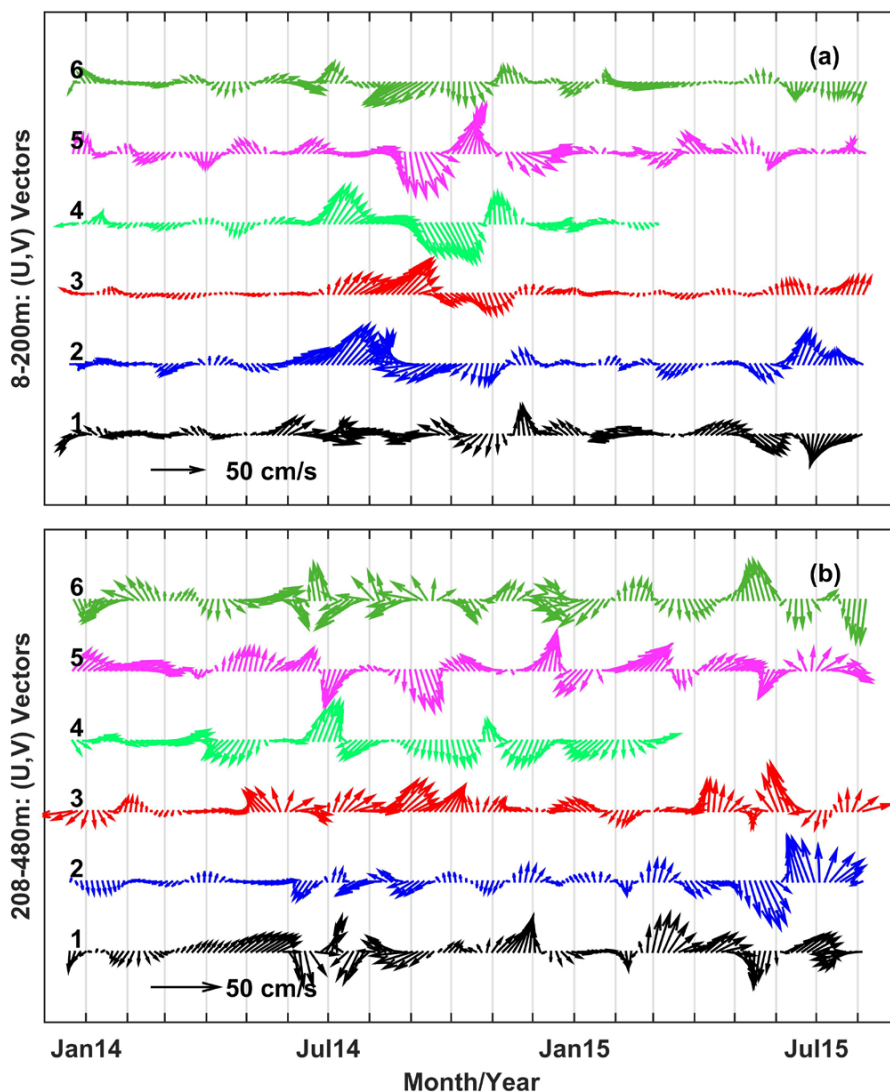


FIGURE 5. Depth-averaged 30-day low-passed filtered currents at mooring locations NRL1–NRL6. (a) Currents averaged between 8 m and 200 m. (b) Currents averaged between 208 m and 480 m. Note that in order to obtain a better presentation of velocity vectors, the vector scale shown in (b) is larger than that in (a).

data is about 0.24 m s^{-1} , which is close to the phase of the second-mode baroclinic Rossby wave at 6°N (Yu 2003; see also Figure 1 in Subrahmanyam et al., 2001). The difference in phase speeds in the present observations near 8°N and in the XBT analysis at 6°N is likely due to the latitudinal dependence on phase speed.

Intraseasonal oscillations (ISOs, varying from 30–90 days) were found in the entire water column, but they were more visible below 200 m, where the magnitude of velocity fluctuations was as large as 0.25 m s^{-1} . Frequency spectra of velocity (not shown here) indicated multiple ISO periods, but the 50–60 day variability was the largest. To examine the ISO energetics, kinetic energy (KE) in the 30- to 90-day band was examined. The time-averaged ISO KE was found to be largest near the surface ($\sim 100\text{--}130 \text{ cm}^2 \text{ s}^{-2}$) and decayed with depth at 100 m and deeper to about $10\text{--}38 \text{ cm}^2 \text{ s}^{-2}$. Preliminary analysis indicates that 30–90 day band-passed filtered SSH anomalies propagated westward with a speed of about 0.2 m s^{-1} (not shown). Girishkumar et al. (2011) showed westward propagation of 40- to 100-day band-passed SSH anomalies at 8°N , 90°E . They suggested their observations are consistent with Rossby wave propagation and noted modulation of the barrier layer as a result of these waves. Girishkumar et al. (2011) further reported that these waves are remotely forced by intraseasonal surface winds in the equatorial Indian Ocean. Several investigators show the existence of 30- to 90-day oscillations in the northeastern BoB, including variations in the EICC transport on intraseasonal time scales (Durand et al., 2009; Mukherjee et al., 2014). Durand et al. (2009) suggest that intraseasonal fluctuations are driven by remote forcing of the equatorial Madden Julian Oscillations. In summer, there appear to be strong northeastward 30–60 day atmospheric oscillations originating from the equator and propagating toward the northern BoB (Kemball-Cook and Wang, 2001). Analyses presented here are preliminary, and

further analysis focusing on the dynamics of these waves and their role in monsoon variability is still required.

SUMMARY

The main objectives of the ASIRI-EBOB field program are to understand and quantify currents, hydrography, mixing, and fresh and salty exchanges between the Southeast Arabian Sea and the Bay of Bengal. The program has provided new insights into deep currents and small-scale, high-frequency variability, some of which had not been observed in the southern BoB before. Long-term time series of velocity, hydrographic, and turbulence fields were collected from six subsurface moorings in the southern BoB.

The moorings were deployed in the deep ocean ($\sim 4,000 \text{ m}$) in December 2013 and recovered in August 2015 using R/V *Roger Revelle*, operating from Sri Lanka. These moorings provided currents between 6 m and 500 m from ADCPs, supplemented by hydrographic data and turbulent dissipation rates at selected depths. During the recovery, we found that the moorings were entangled with commercial fishing lines and nets. The observed large vertical movements ($\sim 150 \text{ m}$) of the moorings are likely due to dragging by the fishing gear. Top subsurface buoys that housed ADCPs were positioned closer to the surface than planned. Regardless of these adverse events, we were lucky to recover almost all the sensors and data.

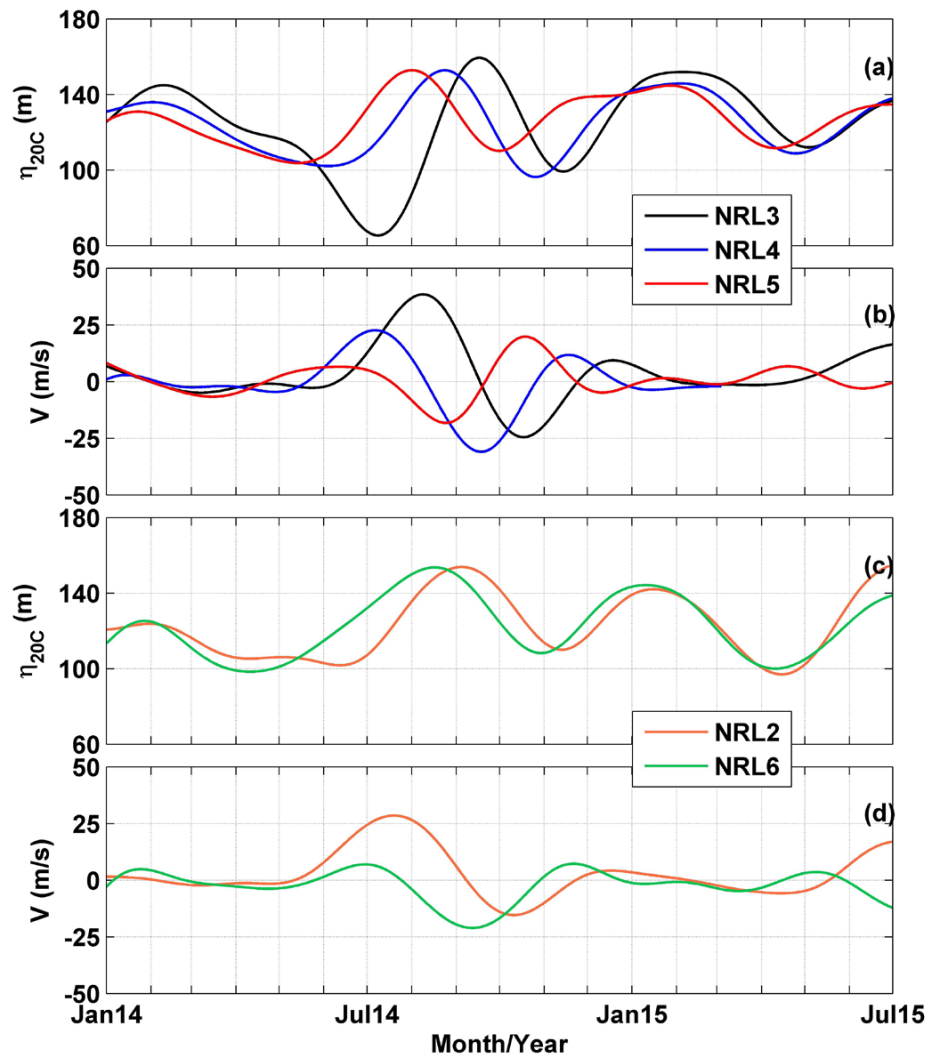



FIGURE 6. Time series of 90-day low-passed filtered 20°C -isotherm depth ($\eta_{20^\circ\text{C}}$), and 8–200 m averaged meridional velocity (V). (a) $\eta_{20^\circ\text{C}}$ and (b) V at NRL3, NRL4, and NRL5. (c) $\eta_{20^\circ\text{C}}$ and (d) V at NRL2 and NRL6.

Moored observations captured the summer and winter monsoon currents, eddies, and intraseasonal oscillations. Near-surface temperature appeared to be warmest during summer but prior to summer monsoons. Near-surface currents as large as 1.75 m s^{-1} were observed in July 2014. Currents

We presented preliminary analyses of moored observations of low-frequency flow fields here. A greater understanding of upper-ocean circulation and its coupling to monsoons will emerge as ongoing analyses of the oceanic and atmospheric data sets along with air-sea coupled model studies are completed. 

“ A greater understanding of upper-ocean circulation and its coupling to monsoons will emerge as ongoing analyses of the oceanic and atmospheric data sets along with air-sea coupled model studies are completed. ”

stronger than 0.5 m s^{-1} were confined to the upper 200 m. Weak time-mean currents below 200 m were dominated by interseasonal oscillations. Moored currents along with drifter deployments show that near-surface flow moved eastward toward the Andaman Sea, indicating that the majority of surface transport was eastward. However, between depths of 50 m and 125 m, the subsurface flow, associated with high-salinity (>35 psu) water, had a strong northward component of about 0.5 m s^{-1} . It is likely that the subsurface-intensified northward component of the flow carried high-salinity water into the northern bay, similar to what has been suggested in past studies. Observations of currents, temperature, and SSH fields revealed eddylike features with positive and negative SSH anomalies (~ 20 cm) moving westward at a speed of about 0.1 m s^{-1} . Intraseasonal oscillations with periods ranging from 30 to 90 days were strongest near the surface. The time-averaged kinetic energy at the ISO band was found to be largest near the surface ($\sim 100\text{--}130 \text{ cm}^2 \text{ s}^{-2}$) and decayed with depth to about $10\text{--}38 \text{ cm}^2 \text{ s}^{-2}$ at 100 m and deeper.

REFERENCES

- Anderson, D.L.T., and P.B. Rowlands. 1976. The role of inertia-gravity and planetary waves in the response of a tropical ocean to the incidence of an equatorial Kelvin wave on a meridional boundary. *Journal of Marine Research* 34:295–312.
- Bhat, G.S., S. Gadgil, P.V. Harish Kumar, S.R. Kalsi, P. Madhusoodanan, V.S.N. Murty, C.V.K. Prasada Rao, V. Ramesh Babu, L.V.G. Rao, R.R. Rao, and others. 2001. BOBMEX: The Bay of Bengal Monsoon Experiment. *Bulletin of the American Meteorological Society* 82:2,217–2,243, [http://dx.doi.org/10.1175/1520-0477\(2001\)082<2217:BTBOBM>2.3.CO;2](http://dx.doi.org/10.1175/1520-0477(2001)082<2217:BTBOBM>2.3.CO;2).
- Cane, M.A., and E.S. Sarachik. 1976. Forced baroclinic ocean motions: Part 1. Linear equatorial unbounded case. *Journal of Marine Research* 34:629–665.
- Durand, F., D. Shankar, F. Birol, and S.S.C. Shenoi. 2009. Spatiotemporal structure of the East India Coastal Current from satellite altimetry. *Journal of Geophysical Research* 114, C02013, <http://dx.doi.org/10.1029/2008JC004807>.
- Girishkumar, M.S., M. Ravichandran, and M.J. McPhaden. 2013. Temperature inversions and their influence on the mixed layer heat budget during the winters of 2006–2007 and 2007–2008 in the Bay of Bengal. *Journal of Geophysical Research* 118:2,426–2,437, <http://dx.doi.org/10.1002/jgrc.20192>.
- Girishkumar, M.S., M. Ravichandran, M.J. McPhaden, and R.R. Rao. 2011. Intraseasonal variability in barrier layer thickness in the south central Bay of Bengal. *Journal of Geophysical Research* 116, C03009, <http://dx.doi.org/10.1029/2010JC006657>.
- Jensen, T.G. 2001. Arabian Sea and Bay of Bengal exchange of salt and tracers in an ocean model. *Geophysical Research Letters* 28(20):3,967–3,970, <http://dx.doi.org/10.1029/2001GL013422>.
- Jensen, T.G. 2003. Cross-equatorial pathways of salt and tracers from the northern Indian Ocean: Modelling results. *Deep Sea Research Part II* 50(12–13):2,111–2,127, [http://dx.doi.org/10.1016/S0967-0645\(03\)00048-1](http://dx.doi.org/10.1016/S0967-0645(03)00048-1).
- Kemball-Cook, S., and B. Wang. 2001. Equatorial waves and air–sea interaction in the boreal summer intraseasonal oscillation. *Journal of Climate* 14:2,923–2,942, [http://dx.doi.org/10.1175/1520-0442\(2001\)014<2923:EWAASI>2.0.CO;2](http://dx.doi.org/10.1175/1520-0442(2001)014<2923:EWAASI>2.0.CO;2).
- Lucas, A.J., E.L. Shroyer, H.W. Wijesekera, H.J.S. Fernando, E. D’Asaro, M. Ravichandran, S.U.P. Jinadasa, D. Sengupta, J.A. MacKinnon, J.D. Nash, and others. 2014. Mixing to monsoons: Air–sea interactions in the Bay of Bengal. *Eos, Transactions American Geophysical Union* 95:269–276, <http://dx.doi.org/10.1002/2014EO300001>.
- McCreary, J.P., W. Han, D. Shankar, and S.R. Shetye. 1996. Dynamics of the East India Coastal Current: Part 2. Numerical solutions. *Journal of Geophysical Research* 101:13,993–14,010, <http://dx.doi.org/10.1029/96JC00560>.
- McPhaden, M.J., G. Meyers, K. Ando, Y. Masumoto, V.S.N. Murty, M. Ravichandran, F. Syamsudin, J. Vialard, L. Yu, and W. Yu. 2009. RAMA: The Research Moored Array for African–Asian–Australian Monsoon Analysis and Prediction. *Bulletin of the American Meteorological Society* 90:459–480, <http://dx.doi.org/10.1175/2008BAMS2608.1>.
- Moum, J.N., and J.D. Nash. 2009. Mixing measurements on an equatorial ocean mooring. *Journal of Atmospheric and Oceanic Technology* 26:317–336, <http://dx.doi.org/10.1175/2008JTECHO6171>.
- Mukherjee, A., D. Shankar, V. Fernando, P. Amol, S.G. Aparna, R. Fernandes, G.S. Michael, S.T. Khalap, N.P. Satelkar, Y. Agarvadekar, and others. 2014. Observed seasonal and intraseasonal variability of the East India Coastal Current on the continental slope. *Journal of Earth System Science* 123(6):1,197–1,232, <http://dx.doi.org/10.1007/s12040-014-0471-7>.
- Murty, V.S.N., Y.V.B. Sarma, and D.P. Rao. 1996. Variability of the oceanic boundary layer characteristics in the northern Bay of Bengal during MONTBLEX-90. *Proceedings Indian Academy of Science (Earth Planet Science)* 105:41–61, <http://dx.doi.org/10.1007/BF02880758>.
- Murty, V.S.N., Y.V.B. Sarma, D.P. Rao, and C.S. Murty. 1992. Water characteristics, mixing and circulation in the Bay of Bengal during southwest monsoon. *Journal of Marine Research* 50:207–228.
- Perlin, A., and J.N. Moum. 2012. Comparison of thermal dissipation rate estimates from moored and profiling instruments at the equator. *Journal of Atmospheric and Oceanic Technology*, 29:1,347–1,362, <http://dx.doi.org/10.1175/JTECH-D-12-00019.1>.
- Philander, S.G.H. 1990. *El Niño, La Niña and the Southern Oscillation*. Academic Press, 289 pp.
- Potemra, J.T., M.E. Luther, and J.J. O’Brien. 1991. The seasonal circulation of the upper ocean in the Bay of Bengal. *Journal of Geophysical Research* 96:12,667–12,683, <http://dx.doi.org/10.1029/91JC01045>.
- Rao, R.R., M.S. Girish Kumar, M. Ravichandran, A.R. Rao, V.V. Gopalakrishna, and P. Thadathil. 2010. Interannual variability of Kelvin wave propagation in the wave guides of the equatorial Indian Ocean, the coastal Bay of Bengal and the southeastern Arabian Sea during 1993–2006. *Deep Sea Research Part I* 57(1):1–13, <http://dx.doi.org/10.1016/j.dsr.2009.10.008>.
- Rao, R.R., and R. Sivakumar. 2003. Seasonal variability of sea surface salinity and salt budget of the mixed layer of the north Indian Ocean. *Journal of Geophysical Research* 108(C1), 3009, <http://dx.doi.org/10.1029/2001JC000907>.
- Rao, S.A., S.K. Saha, S. Pokhrel, D. Sundar, A.R. Dhakate, S. Mahapatra, S. Ali, H.S. Chaudhari, P. Shreeram, S. Vasimalla, and others. 2011. Modulation of SST, SSS over northern Bay of

- Bengal on ISO time scale. *Journal of Geophysical Research* 116, C09026, <http://dx.doi.org/10.1029/2010JC006804>.
- Schott, F., and J.P. McCreary. 2001. The monsoon circulation of the Indian Ocean. *Progress in Oceanography* 51:1–123, [http://dx.doi.org/10.1016/S0079-6611\(01\)00083-0](http://dx.doi.org/10.1016/S0079-6611(01)00083-0).
- Schott, F., J. Reppin, J. Fisher, and D. Quadfasel. 1994. Currents and transports of the Monsoon Current south of Sri Lanka. *Journal of Geophysical Research* 99(C12):25,127–25,141, <http://dx.doi.org/10.1029/94JC02216>.
- Shankar, D., P.N. Vinayachandran, and A.S. Unnikrishnan. 2002. The monsoon currents in the north Indian Ocean. *Progress in Oceanography* 52:63–120, [http://dx.doi.org/10.1016/S0079-6611\(02\)00024-1](http://dx.doi.org/10.1016/S0079-6611(02)00024-1).
- Shenoi, S.S.C., D. Shankar, and S.R. Shetye. 2002. Differences in heat budgets of the near-surface Arabian Sea and Bay of Bengal: Implications for the summer monsoon. *Journal of Geophysical Research* 107(C6), 3052, <http://dx.doi.org/10.1029/2000JC000679>.
- Shetye, S.R., A.D. Gouveia, D. Shankar, S.S.C. Shenoi, P.N. Vinayachandran, D. Sundar, G.S. Michael, and G. Nampoothiri. 1996. Hydrography and circulation in the western Bay of Bengal during the northeast monsoon. *Journal of Geophysical Research* 101:14,011–14,025, <http://dx.doi.org/10.1029/95JC03307>.
- Subrahmanyam, S., I.S. Robinson, J.R. Blundell, and P.G. Challenor. 2001. Indian Ocean Rossby waves observed in TOPEX/POSEIDON altimeter data and in model simulations. *International Journal of Remote Sensing* 22:1,141–1,167, <http://dx.doi.org/10.1080/014311601750038893>.
- Suresh, I., J. Vialard, M. Lengaigne, W. Han, J. McCreary, F. Durand, and P.M. Muraleedharan. 2013. Origins of wind-driven intraseasonal sea level variations in the North Indian Ocean coastal waveguide. *Geophysical Research Letters* 40:5,740–5,744, <http://dx.doi.org/10.1002/2013GL058312>.
- Vialard, J., S.S.C. Shenoi, J.P. McCreary, D. Shankar, F. Durand, V. Fernando, and S.R. Shetye. 2009. Intraseasonal response of the northern Indian Ocean coastal waveguide to the Madden–Julian Oscillation. *Geophysical Research Letters* 36, L14606, <http://dx.doi.org/10.1029/2009GL038450>.
- Vinayachandran, P.N., Y. Masurnoto, T. Mikawa, and T. Yarnagata. 1999. Intrusion of the Southwest Monsoon Current into the Bay of Bengal. *Journal of Geophysical Research* 104:11,077–11,085, <http://dx.doi.org/10.1029/1999JC900035>.
- Vinayachandran, P.N., D. Shankar, S. Vernekar, K.K. Sandeep, P. Amol, C.P. Neema, and A. Chatterjee. 2013. A summer monsoon pump to keep the Bay of Bengal salty. *Geophysical Research Letters* 40:1,777–1,782, <http://dx.doi.org/10.1002/grl.50274>.
- Vinayachandran, P.N., and T. Yarnagata. 1998. Monsoon response of the sea around Sri Lanka: Generation of thermal domes and anticyclonic vortices. *Journal of Physical Oceanography* 28:1,946–1,960, [http://dx.doi.org/10.1175/1520-0485\(1998\)028<1946:MRO TSA>2.0.CO;2](http://dx.doi.org/10.1175/1520-0485(1998)028<1946:MRO TSA>2.0.CO;2).
- Webster, P.J., E.F. Bradley, C.W. Fairall, J.S. Godfrey, P. Hacker, R.A. Houze Jr., R. Lukas, Y. Serra, J.M. Hummon, T.D.M. Lawrence, and others. 2002. The JASMINE Pilot Study. *Bulletin of the American Meteorological Society* 83:1,603–1,630, <http://dx.doi.org/10.1175/BAMS-83-11-1603>.
- Wijesekera, H.W., T.G. Jensen, E. Jarosz, W.J. Teague, E.J. Metzger, D.W. Wang, U. Jinadasa, K. Arulanathan, L. Centurioni, and H.J.S. Fernando. 2015. Southern Bay of Bengal currents and salinity intrusions during a fall monsoon transition. *Journal of Geophysical Research* 120(10):6,897–6,913, <http://dx.doi.org/10.1002/2015JC010744>.
- Wijesekera, H.W., E. Shroyer, A. Tandon, M. Ravichandran, D. Sengupta, S.U.P. Jinadasa, H.J.S. Fernando, N. Agarwal, K. Arulanathan, G.S. Bhat, and others. In press. ASIRI: An ocean-atmosphere initiative for Bay of Bengal. *Bulletin of the American Meteorological Society*, <http://dx.doi.org/10.1175/BAMS-D-14-00197.1>.
- Wyrtki, K. 1973. An equatorial jet in the Indian Ocean. *Science* 181:262–264, <http://dx.doi.org/10.1126/science.181.4096.262>.
- Yu., L., 2003. Variability of the depth of the 20°C isotherm along 6°N in the BoB: Its response to remote and local forcing and its relation to satellite SSH variability. *Deep Sea Research Part II* 50:2,285–2,304, [http://dx.doi.org/10.1016/S0967-0645\(03\)00057-2](http://dx.doi.org/10.1016/S0967-0645(03)00057-2).
- Yu, L., and M.J. McPhaden. 2011. Ocean pre-conditioning of Cyclone Nargis in the Bay of Bengal: Interaction between Rossby waves, surface fresh waters, and sea surface temperatures. *Journal of Physical Oceanography* 41:1,741–1,755, <http://dx.doi.org/10.1175/2011JPO4437.1>.
- Yu, L., J.J. O'Brien, and J. Yang. 1991. On the remote forcing of the circulation in the Bay of Bengal. *Journal of Geophysical Research* 96:20,449–20,454, <http://dx.doi.org/10.1029/91JC02424>.

ACKNOWLEDGMENTS

This work was sponsored by the US Office of Naval Research (ONR) in an ONR Departmental Research Initiative (DRI), Air-Sea Interactions Regional Initiative (ASIRI), and a US Naval Research Laboratory project, Effects of Bay of Bengal Freshwater Flux on Indian Ocean Monsoon (EBOB). Some of the drifters deployed during ASIRI were funded by National Oceanic and Atmospheric Administration grant #NA10OAR4320156, “The Global Drifter Program.” HJSF and SUPJ were funded by ONR grants N00014-13-1-0199 and N00014-14-1-0279.

AUTHORS

Hemantha W. Wijesekera (hemantha.wijesekera@nrissc.navy.mil) is Oceanographer, **William J. Teague** is Section Head, Oceanographic Processes, **Ewa Jarosz** is Oceanographer, **David W. Wang** is Oceanographer, and **Tommy G. Jensen** is Oceanographer, all at the US Naval Research Laboratory, Stennis Space Center, MS, USA. **S.U.P. Jinadasa** is Head of Division and Principal Scientist, National Aquatic Resources Research and Development Agency, Crow Island, Colombo, Sri Lanka. **Harindra J.S. Fernando** is the Wayne and Diana Murdy Endowed Professor, Department of Civil & Environmental Engineering & Earth Sciences, and Department of Aerospace and Mechanical Engineering, University of Notre Dame, Notre Dame, IN, USA. **Luca R. Centurioni** is Associate Researcher and Principal Investigator of the Global Drifter Program, Scripps Institution of Oceanography, University of California, San Diego, La Jolla, CA, USA. **Zachariah R. Hallock** is Research Scientist, NVision Solutions Inc., Stennis Space Center, MS, USA. **Emily L. Shroyer** is Assistant Professor, College of Earth, Ocean, and Atmospheric Sciences, Oregon State University, Corvallis, OR, USA. **James N. Moum** is Professor, College of Earth, Ocean, and Atmospheric Sciences, Oregon State University, Corvallis, OR, USA.

ARTICLE CITATION

Wijesekera, H.W., W.J. Teague, E. Jarosz, D.W. Wang, T.G. Jensen, S.U.P. Jinadasa, H.J.S. Fernando, L.R. Centurioni, Z.R. Hallock, E.L. Shroyer, and J.N. Moum. 2016. Observations of currents over the deep southern Bay of Bengal—with a little luck. *Oceanography* 29(2):112–123, <http://dx.doi.org/10.5670/oceanog.2016.44>.